

Synthesis and Photoluminescence Study of $Y_2O_3:Eu^{3+}$ and $Y_{2-y-x}Al_yO_3:Eu_x^{3+}$ Nanophosphor

M.A. Patwardhan^{1*}, V. B. Bhatkar² and S.K. Omanwar³

¹Bharati Vidyapeeth's College of Engg. for Women Pune 43(M.S.) INDIA.

²Shri Shivaji Collge Akot(M.S.) 444101 INDIA.

³Department of Physics, SGB Amravati University, Amravati-444602 (M.S.) INDIA.
E-mail: *milindapatwardhan@gmail.com

Abstract

The phosphors of high luminous intensity for flat panel display (FPD), compact fluorescent lamps (CFL) applications must have high purity, single phase uniform particle size and clean surfaces, though lot of work has been carried out on $Y_2O_3:Eu^{3+}$ red nanophosphor, synthesis of nanophosphor with high purity, single phase uniform particle size still remains a challenge. This paper describes synthesis of $Y_2O_3:Eu^{3+}$ and $Y_{2-y-x}Al_yO_3:Eu_x^{3+}$ red nanophosphors by wet chemical and nitrate combustion method and discusses effect of sintering temperature on photoluminescent properties of $Y_{2-y-x}Al_yO_3:Eu_x^{3+}$ in comparison with $Y_2O_3:Eu^{3+}$. Photoluminescence characteristics of $Y_2O_3:Eu^{3+}$ and $Y_{2-y-x}Al_yO_3:Eu_x^{3+}$ nanophosphors for maximal luminescence were investigated through emission spectroscopy, XRD, and scanning electron microscopy.

Keywords: $Y_2O_3:Eu^{3+}$, Red-nanophosphor, And Photoluminescence.

1. Introduction

The phosphor $Y_2O_3:Eu^{3+}$ discovered several years ago is still considered as the best red oxide-phosphor because of its high luminescence intensity, atmospheric stability and the lack of hazardous constituents as opposed to sulphide phosphors. It is widely used in compact fluorescent lamps (CFL) and other display applications [1]. Phosphor particles must have a fine size, narrow size distribution, non aggregation, single phase and spherical morphology for good luminescent characteristic. The phosphor particles prepared by spray pyrolysis have the characteristics of spherical shape, fine size; narrow size distribution, non aggregation and single phase, while the particles prepared

by solid state reaction and aqueous solution methods have irregular and agglomerated shapes. However, the spray pyrolysis has the crucial disadvantage of hollowness of the particles. The hollowness of the particles causes reduction in brightness and long term stability. To solve this problem flame spray pyrolysis was also developed to form the phosphor particles having dense morphology [2]. Hence phosphor particles with spherical shape and filled morphology have been desired for good luminescent properties along with good stability. Introduction of trace quantities of Al^{3+} and B^{3+} ions (added in oxide form) in Y_2O_3 host enhanced sensitivity due to changes in the field strength of the host [3]. Recent interest is concentrated on $\text{Y}_2\text{O}_3:\text{Yb}^{3+}$, Er^{3+} for intense red (up-conversion) emission under 980 nm IR excitation [4]. Effect of metal carbonate fluxes on crystallinity, morphology, and photoluminescence characteristics of $\text{Y}_2\text{O}_3:\text{Eu}^{3+}$ nanophosphor have been well studied [5]. In view of the high cost of $\text{Y}_2\text{O}_3:\text{Eu}^{3+}$, a cheaper alternate to it, is desired. Phosphors that have high conductivity and good luminescence intensity in high voltage range are required for field emissive displays (FEDs). Therefore, one of the constituent of phosphor material has to be a metal such as Zn, Al, Gd etc [3, 6]. In this study quasi-spherical $\text{Y}_{2-y-x}\text{Al}_y\text{O}_3:\text{Eu}_x^{3+}$ red phosphor particles with dense morphology have been prepared by combustion of nitrate mixtures at fairly low temperature 600°C further post treated at 800°C and 1000°C . Its luminescent intensity was found to be increased than that of the same phosphor prepared by same procedure without Al and a comparative study of luminescence intensity under UV excitation is made.

2. Experimental Details

2.1 Synthesis of $(\text{Y}_{1.96}\text{Eu}_{0.04})\text{O}_3$ by Nitrate Combustion method

Chemical decomposition by the action of heat is known as pyrolysis. While in combustion, the reaction products catch fire, in pyrolysis decomposition results in smoke and not fire. $(\text{Y}_{1.96}\text{Eu}_{0.04})\text{O}_3$ was synthesized by nitrate combustion method by adding 2.95 gm Y_2O_3 + 0.093 gm Eu_2O_3 to 200 ml doubled distilled water. The solution becomes milky white. This solution was heated with a magnetic stirrer at 80°C . Nitric acid was added drop wise under constant stirring till transparent solution was obtained. Excess water & nitric acid was evaporated by heating the solution further at 100°C . A white precipitate of nitrates was obtained. This precipitate was mildly ground and 3.4031 gm glycine was added to it in order to make oxidizer to fuel ratio as unity and kept in alumina crucible before being introduced to a furnace preheated at 600°C . White foam like a volcanic eruption was formed. The sample was fast cooled by withdrawing the crucible from the furnace. This foam was crushed into a fine powder which was suspended in Acetone and further sonicated by ultrasonic sonicator for 70 min. The resulting solution had some suspended lighter particles along with sedimented larger particles at the bottom. These suspended lighter particles were collected and dried in oven and used for further characterization viz. XRD, SEM, PL spectra.

2.2 Synthesis of $(Y_{1.92}Al_{0.04}Eu_{0.04})O_3$ by Nitrate Combustion method

The nitrates of Y & Eu are obtained as discussed earlier. To this nitrate solution 0.2 gm $Al(NO_3)_3$ was added. A white precipitate of nitrates was obtained. This precipitate was mildly ground and 3.4031 gm glycine was added to it in order to make oxidizer to fuel ratio as unity and kept in alumina crucible before being introduced to a furnace preheated at $600^\circ C$. White foam like a volcanic eruption was formed. The sample was fast cooled by withdrawing the crucible from the furnace. This foam was crushed into a fine powder which was suspended in Acetone and further sonicated by ultrasonic sonicator for 70 min. The resulting solution had some suspended lighter particles along with sedimented larger particles at the bottom. These suspended lighter particles were collected and dried in oven and post sintered at $600^\circ C$, $800^\circ C$ and $1000^\circ C$ for 2 hours. These particles were used for further characterization viz. XRD, SEM, PL spectra.

2.3 Synthesis of $(Y_{1.96}Eu_{0.04})O_3$ by Wet precipitation method

$(Y_{1.96}Eu_{0.04})O_3$ was synthesized by Wet precipitation method by adding 2.95 gm Y_2O_3 + 0.093 gm Eu_2O_3 to 200 ml doubled distilled water. The solution becomes milky white. This solution was heated with a magnetic stirrer at $80^\circ C$. Nitric acid was added drop wise under constant stirring till transparent solution was obtained. Liquid ammonia was added to the above transparent solution drop wise under constant stirring for 3 hours. Gel-like white precipitate of yttrium hydroxide was formed which was washed with de-ionized water & ethanol 3 to 4 times & dried in an oven at $100^\circ C$ for about 24 hours. This dried precipitate was crushed into a fine powder which was suspended in Acetone and further sonicated by ultrasonic sonicator for 70 min. The resulting solution had some suspended lighter particles along with sedimented larger particles at the bottom. These suspended lighter particles were collected and dried in oven which was used for further characterization viz. XRD, SEM, PL spectra.

3. Results and Discussion

It is known that yttrium occupies two crystallographic sites; 25% S_6 symmetry and 75% C_2 symmetry as illustrated in Fig. 1. Europium atoms can occupy both crystallographic sites; when in the C_2 site the lack of inversion centre allows electric dipole transition particularly the (${}^5D_0 \rightarrow {}^7F_2$) responsible for the red emission at 613 nm. On the contrary, magnetic and electric dipole transitions from the S_6 site are forbidden by the selection rule. Addition of trace quantities of Al^{3+} (added in oxide form) in Y_2O_3 host was found to assist Eu^{3+} in occupying C_2 sites thereby increasing sensitivity for electric dipole transition ${}^5D_0 \rightarrow {}^7F_2$.

Fig. 2 shows the XRD patterns of $Y_{1.92}Al_{0.04}O_3:Eu_{0.04}^{3+}$ by nitrate combustion and sintered at $600^\circ C$, $800^\circ C$, $1000^\circ C$ and $Y_{1.96}O_3:Eu_{0.04}^{3+}$ by nitrate combustion and wet precipitation method respectively. For $Y_{1.96}O_3:Eu_{0.04}^{3+}$ by wet precipitation method two peaks with h k l planes (420) and (332) are seen for 2θ to be 32.5° and 37.7° along with all other major diffraction peaks with [h k l] planes (222), (400), (440), (622) for 2θ to be 28.9° , 33.6° , 48.4° , 57.4° which matches well with those of Y_2O_3 (JCPDS standard no.25-1200).

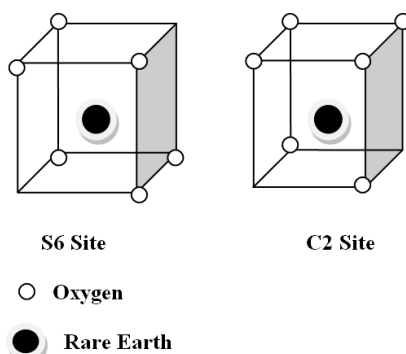


Fig. 1: Symmetry sites for the location of the rare earth atoms in Y_2O_3

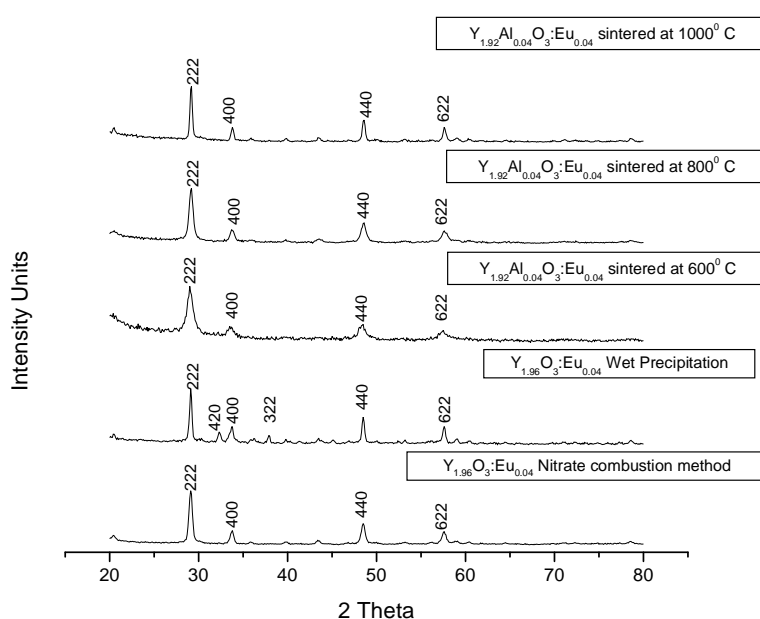


Fig. 2: XRD of $Y_{1.96}Al_{0.04}O_3:Eu^{3+}$ by nitrate combustion and sintered at $600^{\circ}C$, $800^{\circ}C$, $1000^{\circ}C$ and $Y_{1.96}O_3:Eu_{0.04}^{3+}$ by nitrate combustion and wet precipitation method.

While the peaks with h k l planes (420) and (332) which are seen for 2θ to be 32.5° and 37.7° are found to be absent from the diffraction pattern of the samples prepared by nitrate combustion. These observations confirm the strong homogeneity of dopant repartition in the mixed oxides for samples prepared by nitrate combustion as compared to that of Wet chemical method. Diffraction peaks become sharper because of better crystallization at higher sintering temperatures. No other crystalline forms were detected in the XRD pattern of the above samples indicating the formation of cubic phase. The crystallite size of each sample was calculated from the half width of (222) diffraction line of the sample using the Debye Scherrer equation $d = 0.92\{\lambda / (\beta_{1/2} \times \cos\theta)\}$, where d is the diameter of crystallite, λ the wavelength of X-ray, $\beta_{1/2}$ the line width at half maximum in radians and θ the peak angle of the diffraction line. The calculated crystallite sizes were shown in the table 1.1. The crystallite sizes of sample

$Y_{1.92}Al_{0.04}O_3:Eu_{0.04}^{3+}$ varies from 11.19 nm to 27.11 nm as sintering temperature is increased from $600^{\circ}C$ to $1000^{\circ}C$.

Table 1.1: Size of $Y_{1.96}O_3:Eu^{3+}$ and $Y_{1.92}Al_{0.04}O_3:Eu_{0.04}^{3+}$ by XRD.

SN	Sample	Crystallite Size by XRD
1	$Y_{1.96}O_3:Eu^{3+}_{0.04}$ wet precipitation	15.54 nm
2	$Y_{1.96}O_3:Eu^{3+}_{0.04}$ nitrate combustion	13.32 nm
3	$Y_{1.92}Al_{0.04}O_3:Eu_{0.04}^{3+}$ nitrate combustion sintered at $600^{\circ}C$	11.19 nm
4	$Y_{1.92}Al_{0.04}O_3:Eu_{0.04}^{3+}$ nitrate combustion sintered at $800^{\circ}C$	20.47 nm
5	$Y_{1.92}Al_{0.04}O_3:Eu_{0.04}^{3+}$ nitrate combustion sintered at $1000^{\circ}C$	27.11 nm

Table 1.2: Relative PL intensity of $Y_{2-x}O_3:Eu_x^{3+}$ verses Eu concentration.

SN	Eu concentration mol (%)	Relative PL intensity $\lambda_{excitation} = 254\text{ nm}$ $\lambda_{emission} = 613\text{ nm}$
1	0.7	0.46
2	1.6	0.55
3	2.4	0.77
4	4	1.00
5	6.1	0.76

Table 1.2 shows the relative intensity of the sample $Y_{2-x}Eu_xO_3$ for Eu^{3+} concentration in mol% where $0.007 < x < 0.061$. The maximum brightness is obtained at $x = 0.04$. At higher Eu concentration (6.1 mol %) the PL intensity decreases due to concentration quenching [9].

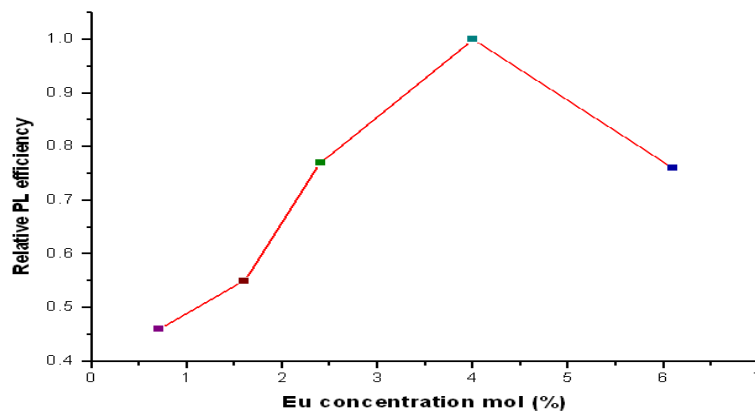


Fig. 3a: Relative PL intensity of $Y_{2-x}O_3:Eu_x^{3+}$ verses Eu concentration.

Table 1.3: Relative PL intensity of $Y_{2-y-x}Al_yO_3:Eu_x^{3+}$ verses Al concentration

SN	Al concentration mol (%)	Relative PL intensity $\lambda_{excitation} = 254 \text{ nm}$ $\lambda_{emission} = 613 \text{ nm}$
1	0.7	0.48
2	1.6	0.55
3	2.4	0.74
4	4	1.00
5	6.1	0.86

Table 1.3 shows the relative intensity of the sample $Y_{2-y-x}Al_yO_3:Eu_x^{3+}$ where y is Al concentration mol% and $0.007 < y < 0.061$ and x is Eu concentration mol%. The maximum brightness is obtained at x = 0.04 and y = 0.04. At higher Al concentration (6.1 mol %) the PL intensity decreases due to concentration quenching.

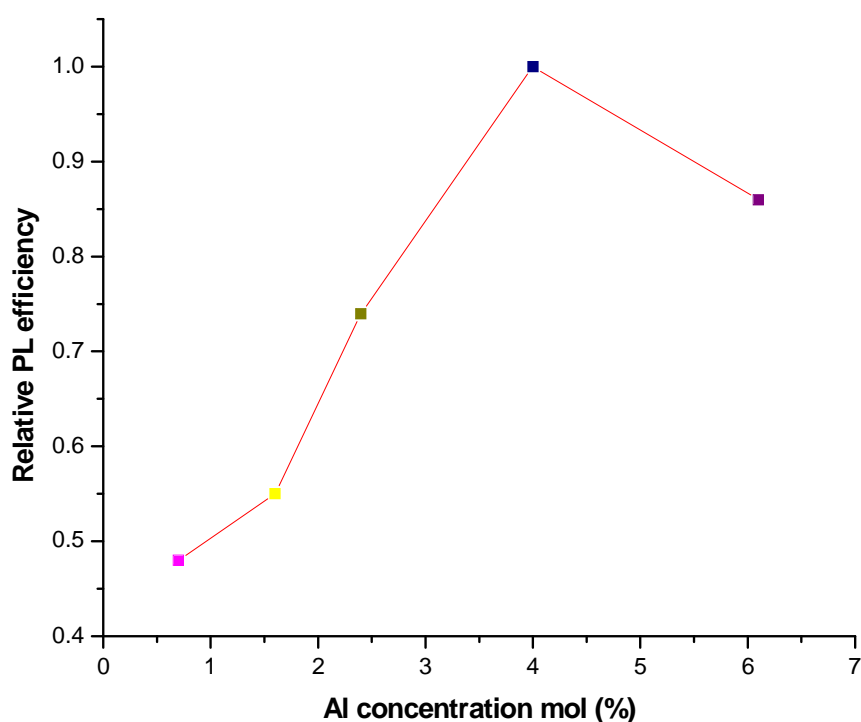
**Fig. 3b:** Relative PL intensity of $Y_{2-y-x}Al_yO_3:Eu_x^{3+}$ verses Al concentration.

Table 1.4 shows comparison of relative PL intensity of $Y_{1.96}O_3:Eu_{0.04}^{3+}$ by nitrate combustion, wet precipitation and $Y_{1.92}Al_{0.04}O_3:Eu_{0.04}^{3+}$ by nitrate combustion sintered at $600^{\circ}C$, $800^{\circ}C$ and $1000^{\circ}C$. The maximum brightness is obtained for the sample $Y_{1.92}Al_{0.04}O_3:Eu_{0.04}^{3+}$ sintered at $1000^{\circ}C$ with relative PL intensity 1.20 as compared with that of commercial yttria red phosphor with relative PL intensity 1.00.

Table 1.4: Comparison of Relative PL intensity of $Y_{1.96}O_3:Eu_{0.04}^{3+}$ by nitrate combustion, wet precipitation and $Y_{1.96}Al_{0.04}O_3:Eu^{3+}$ by nitrate combustion sintered at $600^{\circ}C$, $800^{\circ}C$ and $1000^{\circ}C$.

SN	Sample	Relative PL intensity $\lambda_{excitation} = 254 \text{ nm}$ $\lambda_{emission} = 613 \text{ nm}$
1	$Y_{1.96}O_3:Eu_{0.04}^{3+}$ wet precipitation	0.28
2	$Y_{1.96}O_3:Eu_{0.04}^{3+}$ nitrate combustion	0.32
3	$Y_{1.92}Al_{0.04}O_3:Eu_{0.04}^{3+}$ nitrate combustion sintered at $600^{\circ}C$	0.48
4	$Y_{1.92}Al_{0.04}O_3:Eu_{0.04}^{3+}$ nitrate combustion sintered at $800^{\circ}C$	0.84
5	$Y_{1.92}Al_{0.04}O_3:Eu_{0.04}^{3+}$ nitrate combustion sintered at $1000^{\circ}C$	1.20
6	Commercial Yittria red phosphor	1.00

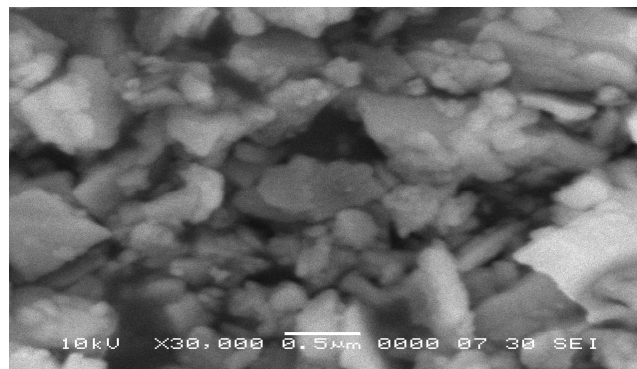


Fig. 4a: SEM micrograph of $Y_{1.96}O_3:Eu_{0.04}^{3+}$ by nitrate combustion.

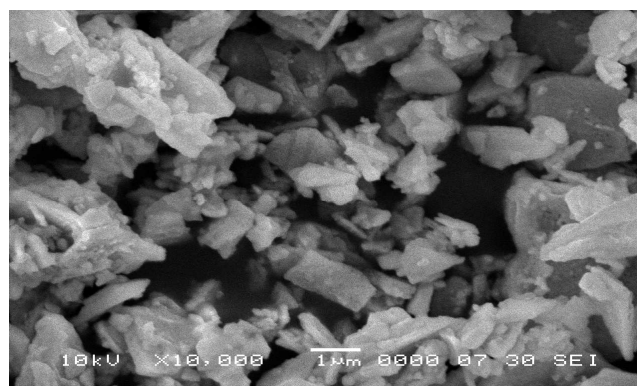


Fig. 4b: SEM micrograph of $Y_{1.92}Al_{0.04}O_3:Eu_{0.04}^{3+}$ by nitrate combustion and sintered at $1000^{\circ}C$.

Fig. 4a and Fig.4b shows SEM micrograph of $Y_{1.96}O_3:Eu_{0.04}^{3+}$ by nitrate combustion and $Y_{1.92}Al_{0.04}O_3:Eu_{0.04}^{3+}$ by nitrate combustion and sintered at $1000^{\circ}C$ respectively in which quasi-spherical particles with filled morphology can be clearly seen.

3.1 Photoluminescence study:

Fig. 5a & 5b shows PL emission spectra of $Y_{1.96}O_3:Eu_{0.04}^{3+}$ by nitrate combustion, wet precipitation and $Y_{1.92}Al_{0.04}O_3:Eu^{3+}$ by nitrate combustion sintered at $600^{\circ}C$, $800^{\circ}C$ and $1000^{\circ}C$ respectively. The Eu^{3+} emission spectra consisted of peaks ranging from 580 nm to 640 nm, which are associated with the transitions from the excited

$^5D_0 \rightarrow ^7F_J$ ($J=0, 1, 2, 3\dots$) with 613 nm ($^5D_0 \rightarrow ^7F_2$) electric dipole transition being the brightest under 254 nm excitation 4f - 4f transition for all the samples but higher sintering temperature lead to better crystallization and result in improved luminescence intensity.

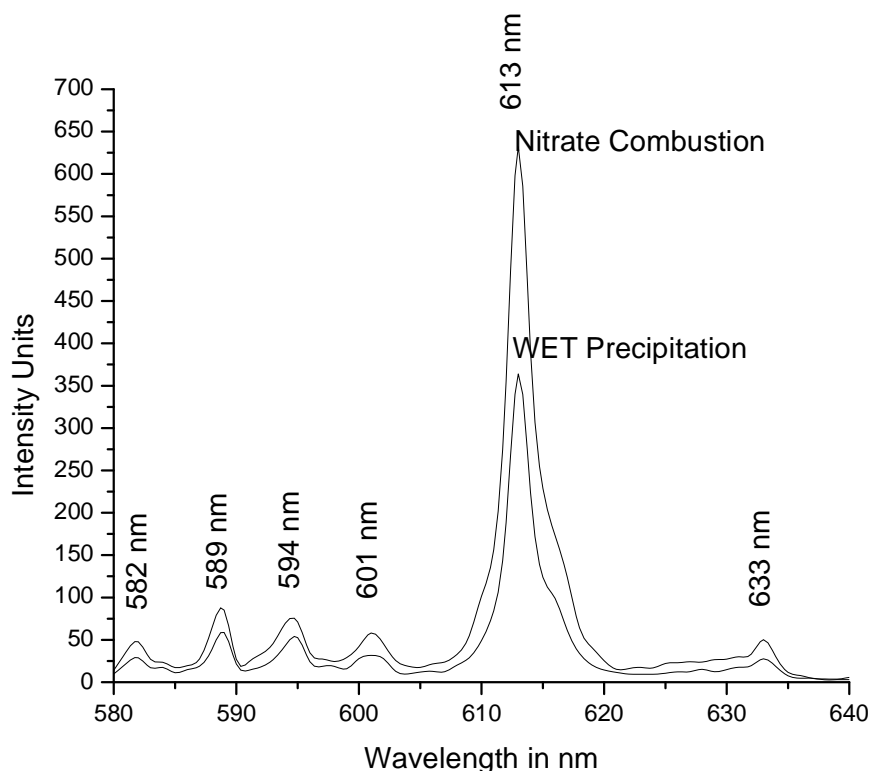


Fig. 5a: PL emission spectra of $Y_{1.96}O_3:Eu_{0.04}^{3+}$ by nitrate combustion, wet precipitation.

Introduction of trace quantities of Al^{3+} (added in oxide form) in Y_2O_3 host enhanced sensitivity due to changes in field strength of host. Hence the 4f-4f transition for $Y_{1.96}Al_{0.04}O_3:Eu_{0.04}^{3+}$ are relatively more intense than $Y_{1.96}O_3:Eu_{0.04}^{3+}$ synthesized by nitrate combustion and wet precipitation [7-8].

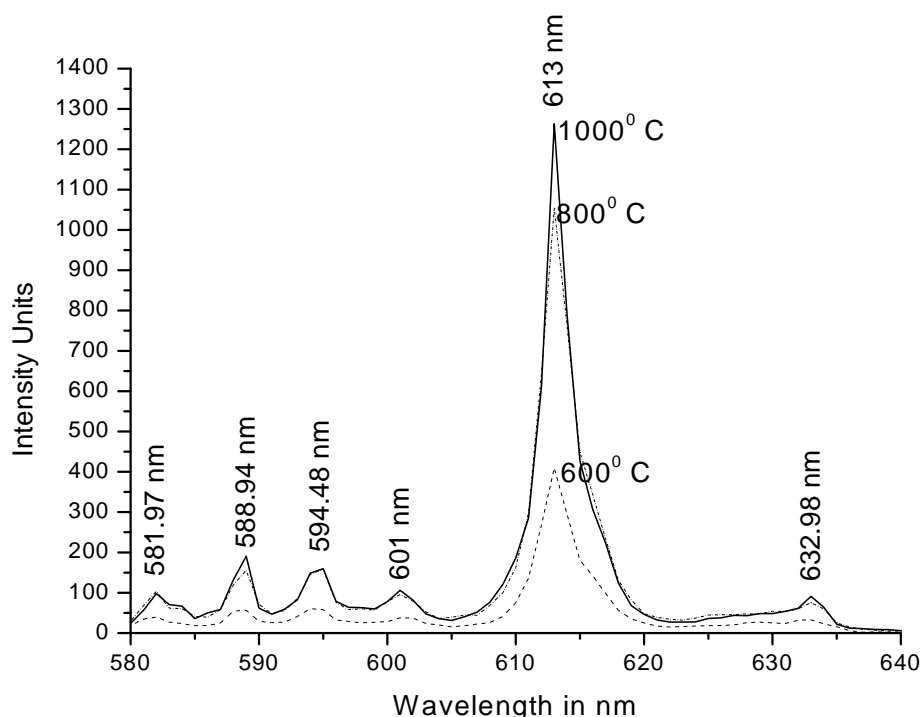


Fig. 5b: PL emission spectra of $Y_{1.92}Al_{0.04}O_3:Eu^{3+}$ by nitrate combustion sintered at $600^\circ C$, $800^\circ C$ and $1000^\circ C$.

4. Conclusion

PL intensity for $Y_{1.96}O_3:Eu_{0.04}^{3+}$ by nitrate combustion method has been found to be increased as compared to by $Y_{1.96}O_3:Eu_{0.04}^{3+}$ wet Precipitation method. PL intensity for $Y_{1.92}Al_{0.04}O_3:Eu_{0.04}^{3+}$ by nitrate combustion method has been found to be increased with the sintering temperatures $600^\circ C$, $800^\circ C$ and $1000^\circ C$ as compared to $Y_{1.96}O_3:Eu_{0.04}^{3+}$ with maximum luminescence intensity for sample sintered at $1000^\circ C$. Introduction of trace quantities of Al (added in oxide form) in Y_2O_3 host enhanced sensitivity due to changes in field strength of host [7-10]. SEM micrograph of $Y_{1.96}O_3:Eu_{0.04}^{3+}$ by nitrate combustion and $Y_{1.92}Al_{0.04}O_3:Eu_{0.04}^{3+}$ by nitrate combustion and sintered at $1000^\circ C$ shows quasi-spherical particles with filled morphology desired for good luminescent properties along with good stability. The intensity of emission peak especially the 613 nm ($^5D_0 \rightarrow ^7F_2$) electric dipole transition being the brightest under 254 nm excitation $4f - 4f$ transition for all the samples but higher sintering temperature lead to better crystallization and result in improved luminescence intensity.

5. Acknowledgement

We are grateful to Dr. D. S. Bilgi, Principal Bharati Vidyapeeth's College of Engineering for Women Pune for constant encouragement. We are also grateful to the Dept. of Physics University of Pune for SEM & XRD measurements.

References

- [1] Nayak A, Goswami K, Ghosh A, Debnath R, *Indian J Pure & Appl Phys*, 47 (2009) 775.
- [2] M.A.Lim, Y.C.Kang, H.D.Park, *Journal of Electrochemical Society*, 148 (2001) H171-H175.
- [3] V Sivakumar, Arunachalam Lakshmanan, R Satheesh Kumar, S Kalpana, R Sangeetha Rani, M T Jose, *Indian Journal of Pure & Applied Physics*, 50 (2012) 123-128.
- [4] Tan C, Liu Y, Han Y, Li W, *J Lumin*, 131 (2011) 1198.
- [5] Y.C.Kang, H.S.Roh, D.J.Seo, S.B.Park, *Journal of Material Science letters*, 19 (2000) 1225-1227.
- [6] Baea J S, Shimb K S, Kimb S B, Jeongb, J H, Yic S S & Park J C, *J Cryst Growth*, 264 (2004)290.
- [7] P.Maestro, D.Huguenin, A.Seigneurin and F. Deneuve, *Journal of Electrochemical Society*, 139 (1992) 1479-1482.
- [8] Takayuki Hirai, Takashi Hirano and Isao Komasaawa, *Journal of Materials Chemistry*, (2000).
- [9] Gun Young Hong, Byung Soo Jeon, Young Kil Yoo, and Jae Soo Yoo, *Journal of Electrochemical Society*, 148 (2001) H161-H166.
- [10] Song-Ho-Byeon, Mi-Gyeong Ko, Jung-Chul Park, Dong-Kuk Kim, *Chem. Mater*, 14 (2002) 603-608.